Session 2: Cosmic noon

INVITED LECTURE

The role of AGN feedback in the baryon cycle at z ∼ 2

Vincenzo Mainieri[ORCID]

European Southern Observatory, Karl-Schwarzschild-Strasse 2,
Garching bei München, Germany

Abstract. In this proceeding I will summarize our on-going observational campaign to characterize Active Galactic Nuclei (AGN) driven ionized gas outflows at z ∼ 2 and assess their impact on galaxy evolution. The results are mostly derived from a recently completed SINFONI/VLT Large Programme named SUPER, conducted with Adaptive Optics to reach a spatial resolution of ∼2 kpc at z ∼ 2.

Keywords. galaxies: active, galaxies: ISM, galaxies: kinematics and dynamics, galaxies: nuclei, (galaxies:) quasars: emission lines

---

1. Introduction

The study of outflows in the host galaxies of active galactic nuclei (AGN) have moved to the forefront of extra-galactic astronomy in recent years, since they are largely invoked on theoretical works to regulate the growth of galaxies (e.g. King & Pounds 2015 for a review). A crucial cosmic epoch is at $1 < z < 3$, corresponding to the peak of volume-averaged star formation and supermassive black hole (SMBH) accretion in the Universe (e.g., Madau & Dickinson 2014), when the energy injected by the central engine onto the host galaxy is expected to be at its maximum. Indeed, many observational studies have revealed that AGN-driven outflows are common at these redshifts (e.g. Brusa *et al.* 2015; Harrison *et al.* 2016; Kakkad *et al.* 2106; Leung *et al.* 2019; Davies *et al.* 2020). While the presence of these outflows out to galactic (kpc) scales is now undisputed, their impact on the gas content and kinematics of the host galaxy is highly debated. This is directly linked to the fact that having firm estimates for the mass of the outflowing gas (M_{out}) and of the energy associated with these outflows represent a major observational challenge. Determining the physical properties of the outflows requires, especially at high redshift, to make assumption on the outflow geometry, the filling factor of the outflowing gas, and the physical gas properties (e.g. density, metallicity, temperature).

Another highly debated topic in the literature is the physical mechanism responsible for generating and driving such outflows on kpc scales. Popular AGN-driven outflow models predict that the interaction of a nuclear wind with the Inter-Stellar Medium (ISM) will generate a reverse shock (Zubovas & King 2012; King & Pounds 2015). In the so-called momentum driven case, the shock cools efficiently and the velocity will decrease constantly with radius. In the energy-driven case, the energy injected by the nuclear wind is conserved and the outflow velocity remains high out to large radii.

It will be therefore upmost important to be able to have observations of outflows at z ∼ 2 with enough quality (e.g. spatial resolution, S/N) to minimize the assumptions and therefore the uncertainties on the physical quantities derived, as well as being able
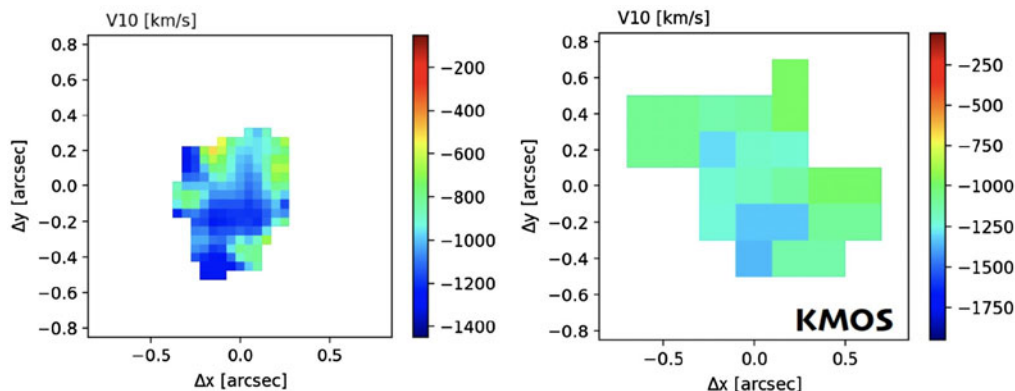
Figure 1. We show the velocity at the 10th percentile of the overall [OIII] line profile (v_{10}) maps for one of the objects in the SUPER survey obtained with SINFONI (*left*) with AO-assisted observations and KMOS (*right*) seeing limited observations in the H band. As it is clear the finer spatial resolution achievable with AO-assisted observations is crucial to have a more detailed characterization of the velocity structures and outflow geometry of the ionized gas, which allow to decrease the uncertainties in the derived quantities, as the mass outflow rate.

to trace the AGN-driven outflows from the proximity of the central SMBH out to the galaxy and possibly Circum-Galactic Medium (CGM) scales to constrain the models. In this proceeding, I will briefly summarize our observational effort to tackle this challenge.

2. The SUPER survey

SUPER† (PI: Mainieri - 196.A-0377) was a Large Programme at the ESO's Very Large Telescope (VLT). The survey has been allocated 280 hours of observing time in AO-assisted mode with the aim of providing high-resolution, spatially-resolved IFS observations of multiple emission lines for a carefully-selected sample of 39 X-ray AGN at z ∼ 2 (Circosta *et al.* 2018). The AO correction is performed in Laser Guide Star-Seeing Enhancer (LGS-SE) mode, which has demonstrated the capability to achieve a point spread function (PSF) full width at half maximum (FWHM) of ∼0.2−0.3 arcsec under typical weather conditions in Paranal. This is a key feature of this survey that allows to resolve the kinematics of the ionized gas to a finer spatial scale than seeing-limited observations, and consequently decrease significantly the uncertainties on the derived physical properties of the detected outflows (see Fig. 1). The sample covers the redshift range of z = 2.1−2.5, which is the epoch of maximal activity of the volume aver-aged star formation in galaxies and the growth of black holes in the universe, making it ideal to study effects of radiative feedback from the black hole on the host galaxy. Thanks to the rich ancillary multi-wavelength data sets available, we were able to derive accu-rate measurements of the black hole and the host galaxy properties via spectral energy distribution fitting of UV-to-FIR photometry and X-ray spectral fitting (Circosta *et al.* 2018; Vietri *et al.* 2018). Of the 39 targets, 22 are classified as Type-1 (56%) and the remaining 17 as Type-2 (44%), based on the presence or absence of broad emission lines such as MgII or CIV in the rest-frame UV spectra. The overall SUPER sample span a wide range in AGN and host galaxy properties which allows us to identify any existing correlation between the outflow properties derived from the SINFONI data and those derived from the multi-wavelength ancillary data set (Circosta *et al.* 2018).
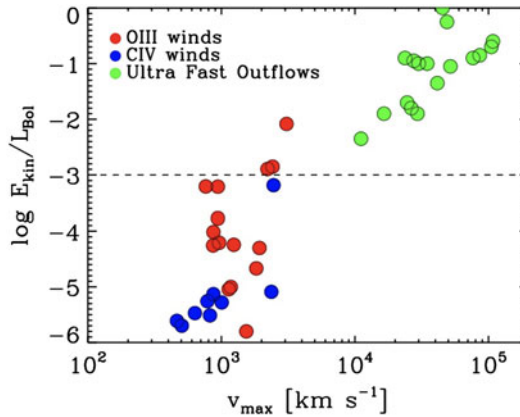
† http://www.super-survey.org

Figure 2. Kinetic coupling efficies obtained for the BLR winds (blue circles), NLR winds (red circles) for the SUPER targets (Vietri *et al.* 2020). We also show a collection of UFOs from Fiore *et al.* (2017). The horizontal dashed line shows the median kinetic coupling efficiency calculated in the simulations presented by Costa *et al.* (2018) (see also Harrison *et al.* 2018).

3. BLR winds

High ionization lines originating from the Broad Line Region (BLR) such as CIV, usually exhibit a shift of the peak to the blue, associated with gas in a non-virial motion (Gaskell 1982; Richards *et al.* 2011; Mejia-Restrepo *et al.* 2018; Vietri *et al.* 2018), which leads to biased estimation of the BH mass. Indeed, this line is known to be dominated by non virialized motions, making the profile asymmetric towards the blue-side of the line. We have therefore the remarkable opportunity to trace the motion of the ionized gas in the BLR (e.g. Vietri *et al.* 2018). In SUPER, we have used the broad Hα and Hβ lines from the SINFONI observations to estimate the radius of the BLR from the BLR radius-luminosity relation (Bentz *et al.* 2009). The inferred radius for the BLR for our AGN at z ∼ 2 is R ∼ 0.1-1 pc. We have measured the velocity shift of the CIV with respect to the laboratory wavelength, which is defined as v_{50}^{CIV}= (λ_{half}-1549.48)*c/1549.48, where λ_{half} is the wavelength that bisects the cumulative total line flux, and c the speed of light. We detected outflow velocities in the BLR up to 5000 km/s (Vietri *et al.* 2020). From those and the radius of the BLR we estimated the kinetic energy associated with these winds. In an attempt to compute the efficiency with which the AGN energy is transfered to the surrounding medium we derived the kinetic coupling efficiecy as the ratio between the kinetic energy and the AGN bolometric luminosity derived from the SED. We show in Fig. 2 the kinetic energy for the BLR and NLR winds from our survey, and a compilation of values for the Ultra-Fast Outflows (UFOs) from Fiore *et al.* (2017). We note that the lower coupling efficiency of BLR winds compared to the UFOs could be due to the combined effect of lower column densisty (N_H) and lower covering factor of the CIV outflowing gas. As discussed also in Harrison *et al.* (2018) the observed values of kinetic coupling efficiency for ionized outflows are lower than the energy injicition rate predicted by simulations, but this should be expected since a portion of the nuclear energy will be used to e.g. work against the gravitational potential.

4. NLR winds

We now move to trace the kinematics of the ionized gas on kpc scales using the [OIII]λ5007 line sampled with AO-assisted SINFONI observations in the H band (Kakkad *et al.* 2020). As it is detailed in the Kakkad *et al.* contribution to these proceedings,
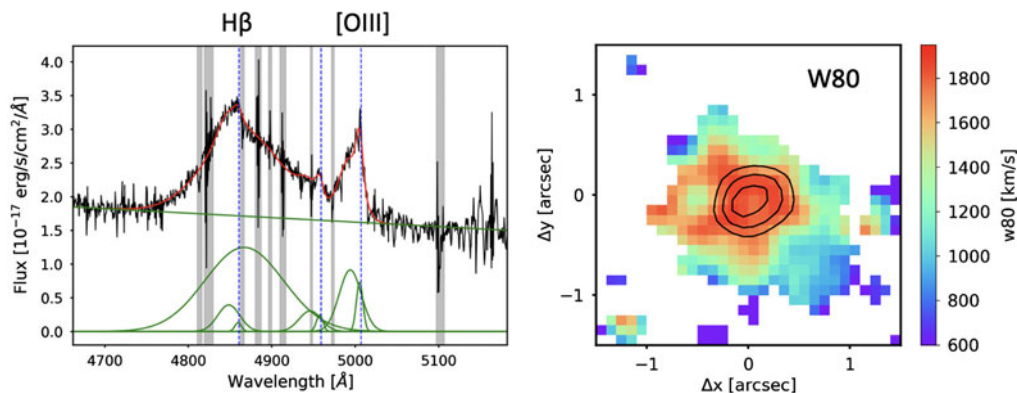
Figure 3. *Left panel:* an example of the H-band integrated spectra from the SUPER survey. The black curve shows the observed spectrum, the red curve shows the best model to reproduce the overall emission, the blue dashed curve shows the iron emission and the green curves show the continuum emission and the individual Gaussian components (Narrow, Broad and BLR) used to reproduce the profiles of various emission lines. The vertical grey regions mark the channels with strong sky lines which were masked during the fitting procedure. *Right panel:* an example of the velocity width (w_{80}) map.

we first verified that the [OIII] emission was actually extended taking into account beam smearing effects (Husemann *et al.* 2016; Villar-Martin *et al.* 2016). We used two techniques to asses if the emission is truly extended. The first consists in comparing the curve-of-growth (COG) of the total [OIII] emission of the AGN with that of an observed and modeled PSF. The second technique, which we called "PSF-subtraction" method, consists in producing a residual [OIII] map after subtracting the nuclear [OIII] spectrum spaxel-by-spaxel following a 2D PSF profile (see also Carniani *et al.* 2015). We found that ≈60% of the Type-1 AGN with S/N (OIII)> 5 present kiloparsec-scale extended ionized gas emission. Flux and velocity maps of these resolved targets reveal outflows extended to kiloparsec scales, with indications of redshifted outflows in three objects. To study the [OIII] line profile properties spaxel-by-spaxel we adopted non-parametric measures, whose have the advantage that the parameter values do not depend on the fitting function adopted (e.g. the number of Gaussian components) that may strongly depend on the signal-to-noise of the spectrum under investigation (see e.g. Zakamska *et al.* 2014; Harrison *et al.* 2014 for more details). In particular, we measure the velocity width of the line that contains 80% of the line flux ($w_{80} = v_{90} - v_{10}$). Using a cut on $w_{80} > 600$ km/s, in the integrated spectra, we found that all the Type-1 AGN in the SUPER survey shows the presence of ionized outflows. The w_{80} maps (see Fig. 3 for an example) show a wide variety of structures and morphologies. A detailed kinematical modeling is on-going to properly characterize the different velocity components in these AGN hosts, and constrain the geometry of the outflow.

5. CO gas content

Finally, a promising way to assess the impact that such detected AGN outflows may have on the ability of the host galaxy to form new stars, may consist in assessing their impact on the moleacular gas reservoir. At the moment there is no consensus in the literature on this topic. Most local studies report no clear evidence for AGN to affect the ISM component of the host, by tracing the molecular phase (e.g. Husemann *et al.* 2017; Saintonge *et al.* 2017; Rosario *et al.* 2018), the atomic one (Ellison *et al.* 2019), and the dust mass as a proxy of the gas mass (Shangguan *et al.* 2019). AGN appear to follow the
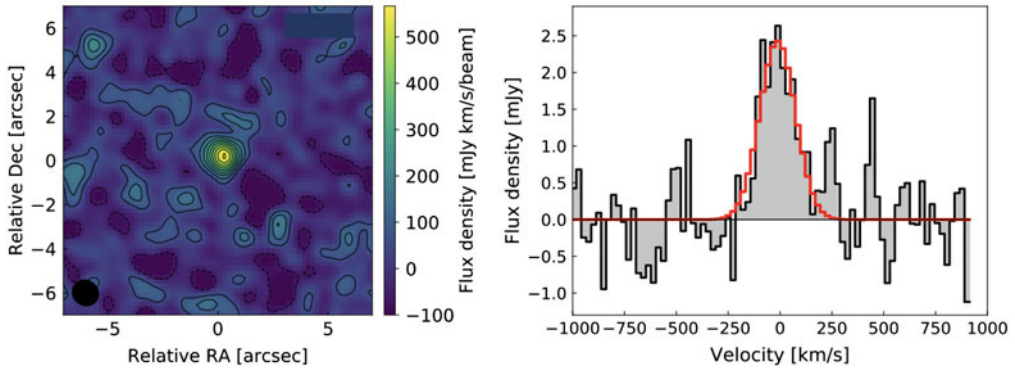
Figure 4. CO line emission maps (*left*) and spectra (*right*) extracted from the region above 2σ significance. Contours are in steps of one sigma for the left panels. On the right, the observed spectrum is plotted in black while the Gaussian model used to fit the spectrum is depicted in red.

same star-formation law of normal galaxies. On the other hand, studies at redshift $z > 1$ present opposite results. In particular, some found reduced molecular gas fractions (i.e., the molecular gas mass per unit stellar mass, $f_{\rm gas} = M_{\rm mol}/M_*$) and depletion timescales of AGN compared with the parent population of normal galaxies (e.g. Kakkad *et al.* 2106; Fiore *et al.* 2017; Brusa *et al.* 2018; Perna *et al.* 2018). This has been interpreted as an evidence for highly efficient gas consumption possibly related to AGN feedback affecting the gas reservoir of the host galaxies. It is hard to directly compare all these studies, both at low and high redshift, given the different selection functions of the sample considered and the different techinque used to asses the molecular gas content in the host. As part of SUPER, we have started a systematic and uniform analysis of the molecular gas content of $z \sim 2$ AGN to infer whether their activity affects the ISM of the host galaxy (Circosta *et al.* 2020; see Fig. 4). As a tracer, we use the CO(3-2) emission line, which is the lowest-J transition accessible with ALMA at $z \sim 2$. We compare the CO emission properties of our AGN as traced by ALMA with those of star-forming galaxies. We have selected a stellar mass and SFR matched sample of comparison galaxies and limited to objects observed in the same CO transition to avoid further uncertainties introduced to the unknown spectral line energy distributions (SLEDs) for these objects.

By comparing the CO and FIR luminosities of our AGN and the control sample, as well as their stellar masses, we found that AGN are overall underluminous in CO. We quantified the CO deficit by: 1) performing a linear fit in the $L'_{\rm CO}$-$L_{\rm FIR}$ plane; 2) dividing our samples in bins of stellar mass and computing mean CO luminosities for each bin; 3) deriving the mean distribution of $L'_{\rm CO}/M_*$ (a proxy of gas fraction) for both samples. We interpreted this finding as an evidence for the effect of AGN activity, which may be able to excite, dissociate or deplete the gas reservoir of the host galaxies.

6. Conclusions

SUPER represents a major advancement in the systematic studies of AGN-driven outflows at a crucial cosmic epoch , $1 < z < 3$, corresponding to the peak of volume-averaged star formation and supermassive black holes accretion in the Universe. The ionized gas kinematics need to be complemented with a significant investment of ALMA time to trace the molecular phase of the outflows (e.g. Cicone *et al.* 2018). The coming years will see the development of facilites that will allow to extend such studies to higher redshift (e.g. the NIRSPec IFU on board of JWST) or to fainter magnitudes and higher spatial resolution (e.g HARMONI at the E-ELT). Finally, it will be very important to invest

substantial resources in the modeling of the multi gas phases outflows, extending the theoretical studies to lower gas temperature than those of the tracers that are currently available.

References

Bentz, M. C., Peterson, B. M., Netzer, H., *et al.* 2009, *ApJ*, 697, 160
Brusa, M., Bongiorno, A., Cresci, G., *et al.* 2015, *MNRAS*, 446, 2394
Brusa, M., Cresci, G., Daddi, E., *et al.* 2018, *A&A*, 612, 29
Carniani, S., Marconi, A., Maiolino, R., *et al.* 2015, *A&A*, 580, A102
Cicone, C., Brusa, M., Ramos Almeida, C., *et al.* 2018, *NatAs*, 2, 176
Circosta, C., Mainieri, V., Padovani, P., *et al.* 2018, *A&A*, 620, A82
Circosta, C., Mainieri, V., Lamperti, I., *et al.* 2020, e-prints, arXiv:2012.07965
Costa, T., Rosdahl, J., Sijacki, D., *et al.* 2018, *MNRAS*, 479, 2079
Davies, R. L., Foerster Schreiber, N. M., Lutz, D., *et al.* 2020, *ApJ*, 894, 28
Ellison, S. L., Brown, T., Catinella, B., *et al.* 2019, *MNRAS*, 482, 5694
Fiore, F., Feruglio, C., Shankar, F., *et al.* 2017, *A&A*, 601, A143
Gaskell, C. M. 1982, *ApJ*, 263, 79
Harrison, C. M., Alexander, D. M., Mullaney, J. R., *et al.* 2014, *MNRAS*, 441,3306
Harrison, C. M., Alexander, D. M., Mullaney, J. R., *et al.* 2016, *MNRAS*, 456,1195
Harrison, C. M., Costa, T., Tadhunter, C. N., *et al.* 2018, *NatAs*, 2, 198
Husemann, B., Scharwaechter, J., Bennert, V. N., *et al.* 2016, *A&A*, 594, A44
Husemann, B., Davis, T. A., Jahnke, K., *et al.* 2017, *MNRAS*, 470, 1570
Kakkad, D., Mainieri, V., Padovani, P., *et al.* 2016, *A&A*, 592, A148
Kakkad, D., Mainieri, V., Vietri, G., *et al.* 2020, *A&A*, 642, A147
King, A. & Pounds, K. 2015, *ARA&A*, 53, 115
Leung, G. C. K., Coil, A. L., Aird, J., *et al.* 2019, arXiv e-prints, arXiv:1905.13338
Madau, P. & Dickinson, M. 2014, *ARA&A*, 52, 415
Mejía-Restrepo, J. E., Lira, P., Netzer, H., *et al.* 2018, *Nature Astronomy*, 2, 63
Perna, M., Sargent, M. T., Brusa, M., *et al.* 2018, *A&A*, 619, 90
Richards, G. T., Kruczek, N. E., Gallagher, S. C., *et al.* 2011, *AJ*, 141, 167
Rosario, D. J., Burtscher, L., Davies, R. I., *et al.* 2018, *MNRAS*, 473, 5658
Saintonge, A., Catinella, B., Tacconi, L. J., *et al.* 2017, *ApJS*, 233, 22
Shangguan, J. & Ho, L. C. 2019, *ApJ*, 873, 90
Vietri, G., Piconcelli, E., Bischetti, M., *et al.* 2018, *A&A*, 617, A81
Vietri, G., Mainieri, V., Kakkad, D., *et al.* 2020, *A&A*, 644, 175
Villar-Martin, M., Arribas, S., Emonts, B., *et al.* 2016, *MNRAS*, 460, 130
Zakamska, N. & Greene, J. E. 2014, *MNRAS*, 442, 784
Zubovas, K. & King, A. 2012, *ApJ*, 745, L34